Properties of train load frequencies and their applications

D.R.M. Milne*, L.M. Le Pen, D.J. Thompson, W. Powrie

Faculty of Engineering and the Environment, University of Southampton, Southampton SO17 1BJ, United Kingdom

*Corresponding Author - d.milne@soton.ac.uk

Abstract

A train in motion applies moving steady loads to the railway track as well as dynamic excitation; this causes track deflections, vibration and noise. At low frequency, the spectrum of measured track vibration has been found to have a distinct pattern; with spectral peaks occurring at multiples of the vehicle passing frequency. This pattern can be analysed to quantify aspects of train and track performance as well as to design sensors and systems for trackside condition monitoring. To this end, analytical methods are developed to determine frequency spectra based on known vehicle geometry and track properties. It is shown that the quasi-static wheel loads from a moving train, which are the most significant cause of the track deflections at low frequency, can be understood by considering a loading function representing the train geometry in combination with the response of the track to a single unit load. The Fourier transform of the loading function describes how the passage of repeating vehicles within a train leads to spectral peaks at various multiples of the vehicle passing frequency. When a train consists of a single type of repeating vehicle, these peaks depend on the geometry of that vehicle type as the separation of axles on a bogie and spacing of those bogies on a vehicle cause certain frequencies to be suppressed. Introduction of different vehicle types within a train or coupling of trainsets with a different inter-car length changes the spectrum, although local peaks still occur at multiples of the passing frequency of the primary vehicle. Using data from track-mounted geophones, it is shown that the properties of the train load spectrum, together with a model for track behaviour, allows calculation of the track system support modulus without knowledge of the axle loads, and enables rapid determination of the train speed. For continuous remote condition monitoring, track-mounted transducers are ideally powered using energy harvesting devices. These need to be tuned to optimise energy abstraction; the appropriate energy harvesting frequencies for given vehicle types and line speeds can also be predicted using the models developed.

Keywords: Track Deflection, Low Frequency Track Vibration, Train Loads, Dominant frequencies, Track Stiffness, Energy Harvesting

1. Introduction

When a train runs along the track it will apply moving steady loads to the track and dynamic excitation due to track unevenness or wheel out-of-roundness. These loads cause vibration, noise and deflections of the track. Understanding the frequency spectrum of track vibration and its relation to train

geometry, loading and sources of excitation and as well as properties of the track, is important for interpreting measurements, explaining vibration and track movement and evaluating track performance. This paper addresses the understanding and interpretation of the spectrum of low frequency track vibration.

At low frequency, spectra of track vibration have a distinct shape in which peaks at certain frequencies are prominent. Several authors have identified that these peaks occur at multiples of the vehicle passing frequency and they have previously been termed 'train load dominant frequencies' [1-6]. Auersch [7] showed that high and low amplitude regions of the spectra are characterised by the axle spacing of a vehicle bogie. Ju et al. [6] showed that the dominant peaks are caused by the repeated loading from vehicles within a train. Ni et al. [8] and Kouroussis at al. [9] demonstrated that this property can be exploited for determining the train speed using the peaks in spectra for track deflection and ground vibration. Jurdic et al. [10] matched the vibration spectrum for the complete train geometry to avoid errors that may arise from the difference between the actual and assumed frequency of the peaks. By considering a model of track deflection in the frequency domain, Le Pen et al. [5] showed that the relative amplitudes of these peaks are influenced by the track stiffness and used this property to obtain the track system support modulus.

Quasi-static loading and dynamic excitation are responsible for track vibration. The quasi-static contribution is from the weight of the train transferred through the suspension system to the track through each wheel, at a steady speed. Dynamic excitation arises from track and wheel unevenness and impact at discontinuities at the wheel/rail interface. The significance of these different mechanisms varies with frequency [11]. Models and measurements by Sheng et al. [12, 13] showed that track deflection from the steady quasi-static loading are the most significant mechanism for low frequency track vibration, whereas dynamic excitation from other mechanisms is usually more significant at higher frequencies. Studies by Lombaert et al. [14], Auersch [7], Triepaischajonsak et al. [15] and Alves-Costa et al. [16] confirm the differing importance of these mechanisms with varying frequency. Furthermore, neglecting wheel unevenness, every wheel will be excited by the same rail roughness leading to the same dynamic load at a point on the track. The time lag between each load, for both the quasi-static and dynamic contributions, is governed by the axle spacing within the train. This leads to a modulation of the low frequency spectrum that is the same for both dynamic and quasi-static loading [17, 18]. This means that quasi-static models for track deflection and the sequence of wheel loads are adequate for interpreting track vibration at low frequency.

In this paper, the Fourier transforms of the response of a beam on an elastic foundation to a point force, a simple analytical model for track deflection, and sequences of applied wheel loads representing different trains are used to explain the frequency and magnitude of the peaks found in measured track vibration spectra. This is done initially for trains consisting of a single repeating vehicle type. It is shown how the relative amplitudes and reliability of the spectral peaks from the wheel load sequence depend on the vehicle geometry. The effects of more complex train geometry, consisting of

multiple vehicle types or coupled trainsets, are also investigated, as is the influence of variation between wheel loads. The significance of these frequencies, their relative amplitudes and their dependence on the properties of the track, is demonstrated with reference to three applications: obtaining the track system support modulus from track deflection measurements , determining the train speed [8-10] and tuning a track-mounted energy harvester for powering transducers for condition monitoring [6]. The insights gained in this paper provide a more rigorous justification for methods used in these three applications by considering the role of the vehicle geometry and the influence of bogie and axle spacing on the shape of track vibration spectra, and the sensitivity of the spectral peaks to the number of vehicles and variation in wheel loads.

2. Low frequency track vibration

2.1. *Track vibration measurements*

Track-mounted vibration transducers such as geophones or accelerometers may be used to record track deflections caused by passing trains [19-24]. In this study, measurements of vertical velocity made on the sleeper have been obtained from different locations with well-performing track using geophones. The train types and vehicle geometries associated with the measurements are given in Table 1. These trains have been categorised according to whether they comprise single or multiple vehicle geometries. Vehicle geometry is described using the vehicle length L_v, bogie spacing L_b and axle spacing L_w. These are shown for twin bogie and articulated vehicle types in Fig. 1.

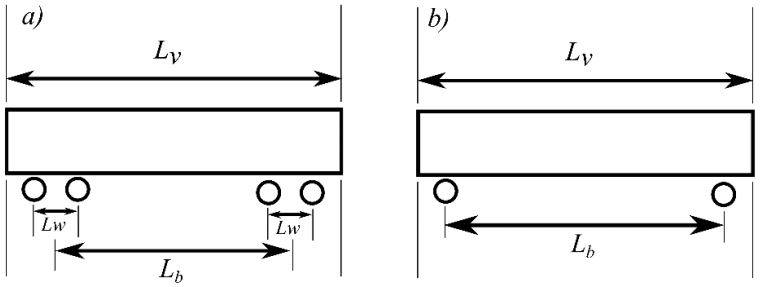

Fig. 1. Typical vehicle geometry: a) twin bogie vehicle, b) articulated vehicle. L_v is the vehicle length, L_b is the bogie spacing and L_w is axle spacing within a bogie.

Table 1 Vehicle geometries considered

Trainset	Vehicle Length L_v	Bogie Spacing L_b	Wheel Spacing L_w
Single Vehicle Geometry			
Electrostar/Javelin	20.0	14.2	2.6
Turbostar/Voyager	23.0	16.0	2.6
Pendolino	23.9	17.0	2.7
Valero	24.8	17.4	2.5
Multiple Vehicle Geometries (*Primary Vehicle Type)			
HST			
Class 43	17.8	10.3	2.6
Mk3 coach*	23.0	16.0	2.6
TGV/Eurostar			
Power car	22.2	14.8	3.0
End car	21.9	18.7	3.0
Articulated car*	18.7	15.7	-

Fig. 2 shows frequency spectra obtained from sleeper velocity measurements for trains having a single vehicle type. The sleeper velocity was measured using geophones in each case and sampled at 500 Hz. The spectra shown are the magnitudes of the Fourier transforms of these signals over a 20 s duration, giving a frequency resolution of 0.05 Hz. The measurements are for the passage of a 6 car Javelin, a 5 car Voyager, an 11 car Pendolino and a 16 car Valero. The corresponding train speeds were 56.4, 56.1, 54.4 and 80.8 m/s. The frequency axis has been non-dimensionalised by the vehicle passing frequency $f_1=v/L_v$ giving $N=f/f_1$ where f is frequency in Hz and v is the speed of the train. The vehicle passing frequencies in these examples are 2.82, 2.44, 2.27 and 3.26 Hz respectively.

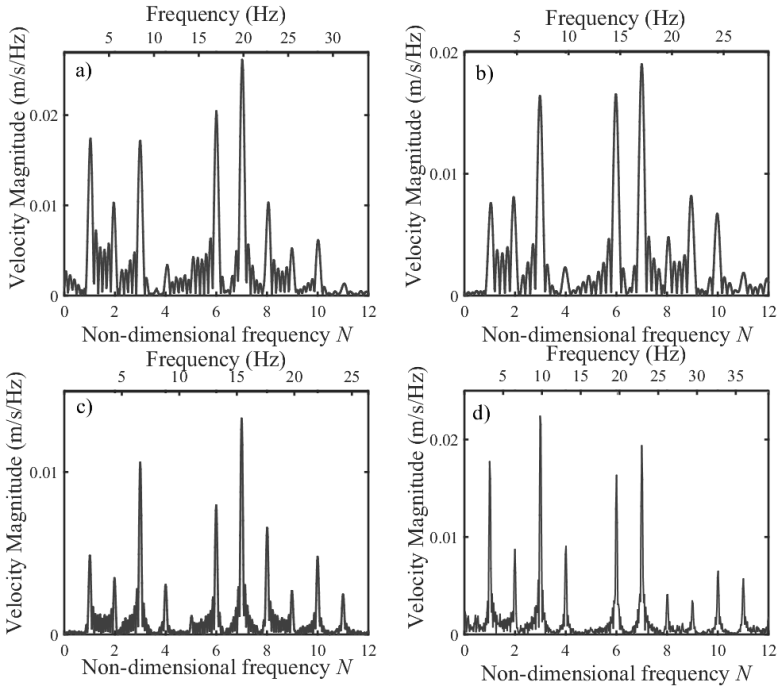

Fig. 2. Magnitude of the Fourier transform of measured sleeper velocities. a) 6 car Javelin (56.4 m/s); b) 5 car Voyager (56.1 m/s); c) 11 car Pendolino (54.4 m/s); d) 16 car Valero (80.8 m/s).

Peaks in the sleeper velocity spectrum correspond to integer multiples of the vehicle passing frequency. However certain multiples are suppressed, such as N=4 and 5 for the Javelin in Fig 2(a). The peaks for the shorter trains with 5 and 6 vehicles (Fig. 2(a, b)) are broader and the spectra show clear subsidiary maxima between the main peaks. The spectral peaks for longer trains with 11 and 16 vehicles (Fig. 2(c, d)) are narrower and more prominent.

Some trains, such as the HST and TGV/Eurostar, comprise different vehicle types (see Table 1); others comprise two or more trainsets joined together with a coupling length different from that within each trainset. Sleeper velocity spectra are given for examples of such trains in Fig. 3. The non-dimensional frequency is based on the length of the most common (primary) vehicle in the train.

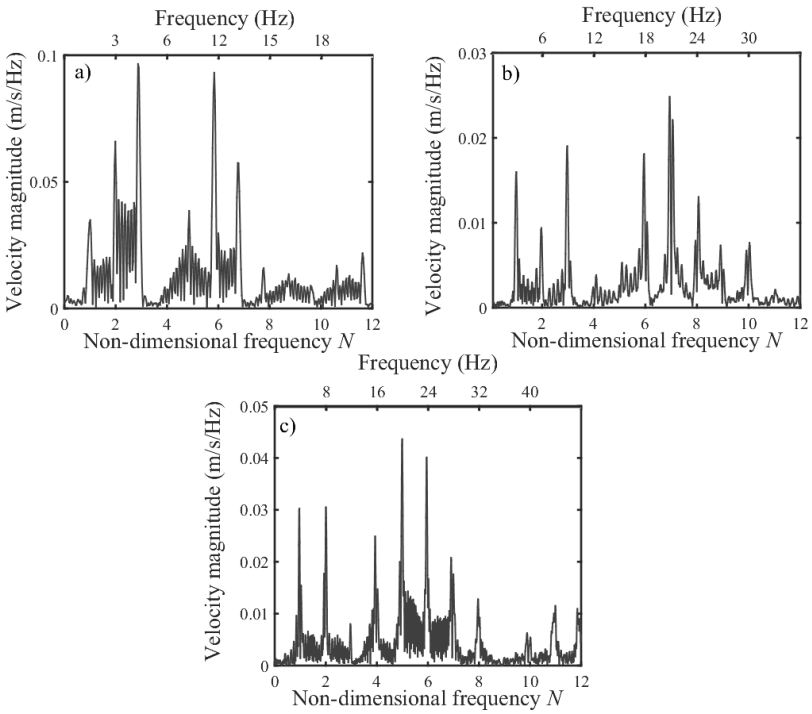

Fig. 3. Magnitude of the Fourier transform for a sleeper velocity: a) 9 vehicle HST (34.5 m/s), b) 12 vehicle Javelin (60 m/s) c) 20 vehicle Eurostar (74.2 m/s).

The spectra in Fig. 3 are similar to those in Fig. 2, with the main spectral peaks occurring at multiples of the vehicle passing frequency for the primary vehicle type from each train. There is more frequency content between the dominant frequencies in Fig. 3 than in Fig. 2, giving the impression of greater noise.

As will be shown, the shape of the measured spectra depends on the vehicle geometry, the number of vehicles and the deflection characteristics of the track.

2.2. *Influence of the track*

Models of the track and sequences of loads can be used to interpret measured vibration as discussed in [5]. As the low frequency behaviour (below 30-40 Hz) is the main focus of the current work, track-train interaction and other dynamic effects can be neglected and a simple Euler-Bernoulli beam formulation is acceptable for the rail [11].

A quasi-static model of a beam on an elastic foundation, in which inertial effects are neglected, is commonly used to represent the deflection of railway track at low frequency. The governing equations are well-known in the literature, e.g. [25]. The solution for displacement w varying with time t at a point on a rail with bending stiffness EI, on a uniform elastic foundation with a system support modulus k, subject to a train of moving loads P_n, each separated from the first load by a distance x_n, is:

$$w(t) = \sum_n \frac{P_n}{2kL} \mathrm{e}^{-\frac{v\left|t-\frac{x_n}{v}\right|}{L}} \left(\cos\left(\frac{v\left|t-\frac{x_n}{v}\right|}{L} \right) + \sin\left(\frac{v\left|t-\frac{x_n}{v}\right|}{L} \right) \right) \quad (1)$$

where L is the effective length:

$$L = \sqrt[4]{\frac{4EI}{k}} \tag{2}$$

Eq.(1) is a convolution of the solution for a single unit moving load $s(t)$ and a sequence of point loads $f(t)$ representing the wheel loads of a train [5]. This convolution corresponds to a product in the frequency domain.

$$W(f) = S(f)F(f) \tag{3}$$

where $S(f)$ and $F(f)$ are the Fourier transforms of $s(t)$, and $f(t)$, respectively. These are referred to as the shape and load spectra and the shape and load functions [5], and are important for understanding and interpreting measurements of low frequency track vibration. The shape spectrum $S(f)$ is found from:

$$\begin{aligned} S(f) &= \frac{1}{2kL}\int_{-\infty}^{\infty} \mathrm{e}^{-\frac{v|t|}{L}}\left(\cos\left(\frac{v|t|}{L}\right)+\sin\left(\frac{v|t|}{L}\right)\right)\mathrm{e}^{-\mathrm{i}2\pi ft}\,\mathrm{d}t \\ &= \frac{4v^3}{4kv^4+16\pi^4kL^4f^4} \end{aligned} \tag{4}$$

The corresponding Fourier transforms for track velocity and acceleration may be obtained by multiplication by $i2\pi f$ and $-4\pi^2f^2$, respectively. Fig. 4(a) shows the track deflection obtained using Eq. 1 for a 50 kN load moving at 50 m/s; for a range of plausible system support moduli. Fig. 4(b) shows the magnitude of the corresponding Fourier transforms normalised by the static load. The frequency axis has been expressed in terms of a non-dimensional vehicle passing frequency for a 20 m long vehicle. These results show the influence of the track stiffness in both the time and the frequency domains. Increasing the track system support modulus shortens the deflection bowl in the space/time domain and increases the higher frequency components in the frequency domain. This is an important property for the applications given later because the shape of a spectrum of measured track vibration depends on the system support modulus.

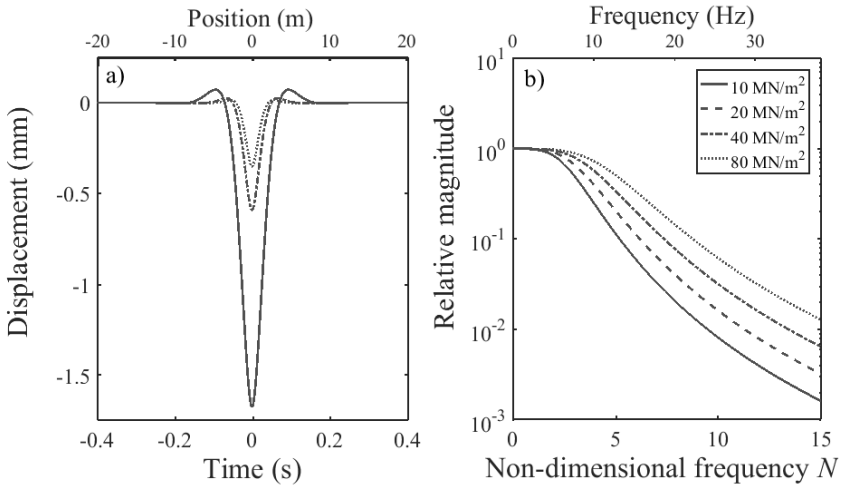

Fig. 4. a) Displacement due to a 50 kN load moving along a single UIC 60 rail at 50 m/s for different system support moduli. b) Magnitude of the Fourier transform of displacement, normalised to static deflection. Non-dimensional frequency corresponds to a 20 m vehicle.

3. Train load spectra

The load function $f(t)$ represents a sequence of wheel loads that are independent of the track. This can be obtained as:

$$f(t) = \sum_n P_n \delta\left(t - \frac{x_n}{v}\right) \tag{5}$$

The Fourier transform of Eq. (5) describes the frequency content of the loading. Which frequencies are most prominent in the load spectrum depends on the geometry of the train and the relative amplitudes of the wheel loads. If the wheel loads are equal, the frequencies and magnitudes depend only on the train geometry.

Trains often comprise repeating vehicles with the same axle configuration, giving periodicity in the loading, see Table 1 and Fig. 2. This type of train may be described as 'periodic'. Initially only periodic trains will be considered as the properties of their Fourier transforms explain certain features in spectra of train loads and simplify their interpretation. Non-periodic geometries are considered in section 3.4. Together sections 3.1-3.4 show the influence of vehicle geometry and train length on the dominant frequencies and their magnitudes. Understanding this improves analysis of track vibration measurements. The equations developed in the following are for twin bogie vehicles (Fig. 1(a)), but can readily be adapted for the simpler case of articulated vehicles (Fig. 1(b)). To illustrate these, examples are given based on Javelin vehicle geometry, which has geometry representative of 20 m long vehicles used in the UK (Table 1).

3.1. *Infinite periodic train with equal wheel loads*

Consider an infinitely long train that consists only of identical repeating vehicles, moving with velocity v. Although the Fourier integral does not converge for an infinite train, the train loads can be represented as a Fourier series because the infinite train is periodic. In this form the frequencies of loading only exist at integer multiples (N) of the vehicle passing frequency. The amplitudes of these discrete frequencies are the Fourier series coefficients, U_N, evaluated over one period of the train, L_v/v. The load function can be written as a Fourier series:

$$f(t) = \sum_{N=-\infty}^{\infty} U_N \mathrm{e}^{-\mathrm{i}2\pi N v t/L_v} \tag{6}$$

where the Fourier series coefficients depend on the vehicle geometry and wheel load P:

$$U_N = 4P\frac{v}{L_v}\cos\left(\frac{\pi N L_b}{L_v}\right)\cos\left(\frac{\pi N L_w}{L_v}\right) \tag{7}$$

Eq. (7) describes the relative amplitude of the discrete train-load frequencies that occur at integer values of N for an infinite train. Fig. 5 shows the magnitude of this (i.e. positive values), with the factor $4Pv/L_v$ omitted, evaluated at the first 12 integer values of N for Javelin vehicle geometry. This function has also been plotted for continuous values of N. Plotting this function for continuous values of N shows how it envelopes the discrete frequencies.

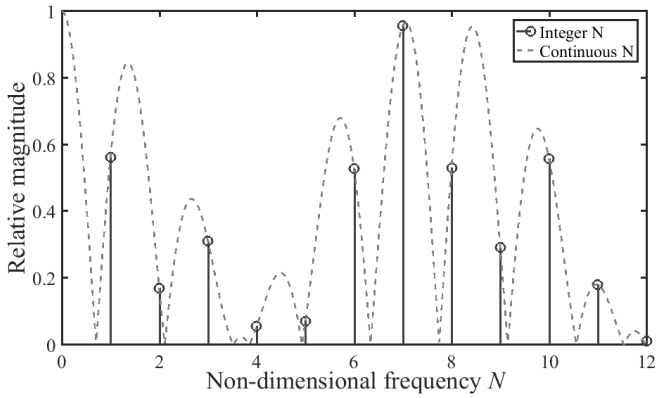

Fig. 5. Discrete load frequencies for an infinite train consisting of 20 m long Javelin vehicles and weighting due to to vehicle geometry

The train loading frequencies of an infinite periodic train are thus discrete and occur at integer multiples of the vehicle passing frequency. However, for a finite length train the trainload spectrum is continuous and obtained from a Fourier transform $F(f)$ rather than a Fourier series. This will now be explored for a single vehicle, a train with an explicit periodic structure and a train that consists of more than one vehicle type.

3.2. *Single vehicle with equal wheel loads*

The train load spectrum for a single vehicle, with four equal wheel loads can be expressed in terms of the non-dimensional vehicle passing frequency N (which is now not necessarily an integer) and the vehicle geometry.

$$F(N) = 4P\cos\left(\frac{\pi N L_b}{L_v}\right)\cos\left(\frac{\pi N L_w}{L_v}\right) \tag{8}$$

The shape of the load spectrum for a single vehicle, Eq. (8) is given by the same function that describes the Fourier series coefficients for an infinite train, Eq. (7). However, Eq. (8) is the continuous train loading spectrum for a single vehicle whereas the mathematically equivalent Eq. (7) weights the discrete frequencies for an infinite train. These expressions depend on the regular wheel separations defined by the axle and bogie spacings. Fig. 6 shows the two cosine functions in these equations and how they combine to form the load spectrum for a single vehicle; for clarity these are shown as magnitudes, i.e. always positive values. For the single vehicle (Fig. 6(c)) the spectral peaks are broad; they do not occur at integer multiples of the vehicle passing frequency, but depend on an interaction between the axle spacing (Fig. 6(a)) and the bogie spacing (Fig. 6(b)). In the spectrum certain frequencies are suppressed; these occur when Eq. (8) is equal to zero, i.e. at $N=rL_v/2L_w$ from the axle spacing and $N=rL_v/2L_b$ for the bogie spacing where r = 1, 3, 5… as described by Auersch [1]. These suppressions that arise from the axle and bogie spacing are periodic in the frequency domain although in general the combined function is not.

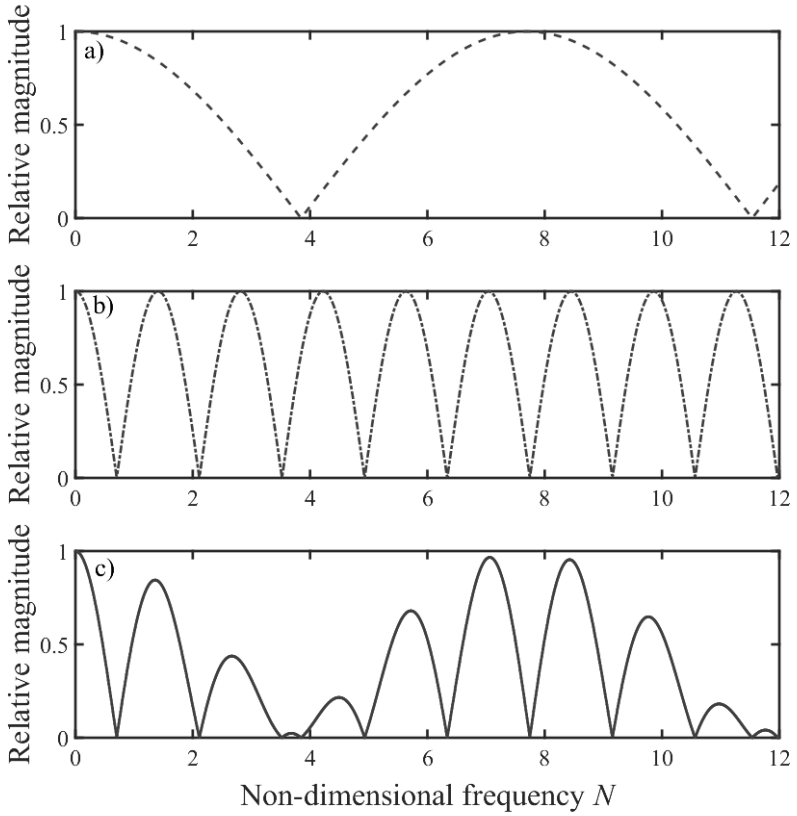

Fig. 6. Components of the single vehicle spectrum a) contribution of axle spacing '- - -' b) contribution of bogie spacing '– · – ' c) single vehicle spectrum '—'for a 20 m Javelin vehicle.

3.3. *Finite 'periodic' trains with equal wheel loads*

For a train consisting of a number of near-identical vehicles, the resulting periodicity gives rise to a train loading spectrum that exhibits properties similar to those for an infinite train. The Fourier transform of the train load function from a train of N_c cars, can be written in terms of the non-dimensional frequency and the vehicle geometry:

$$\mathrm{F}(N) = 4P\cos\left(\frac{\pi N L_b}{L_v}\right)\cos\left(\frac{\pi N L_w}{L_v}\right)\sum_{m=0}^{N_c-1} \mathrm{e}^{-\mathrm{i}2\pi N m} \tag{9}$$

Eq. (9) contains two parts, a weighting function and a series. The weighting function is identical to the spectrum for a single vehicle, Eq. (8), and is found within the function for the Fourier series coefficients for an infinite train, Eq. (7). The axle and bogie spacings are responsible for the suppression of certain frequencies in the spectrum as before.

Fig. 7 shows the magnitude of the series term in Eq. (9) for increasing numbers of vehicles. This implicitly contains information about the train's periodicity. As the number of repeating vehicles within the train increases, the spectral peaks become narrower and occur at integer multiples of the vehicle passing frequency. For N_c vehicles there are $N_c - 1$ subsidiary peaks between each main peak.

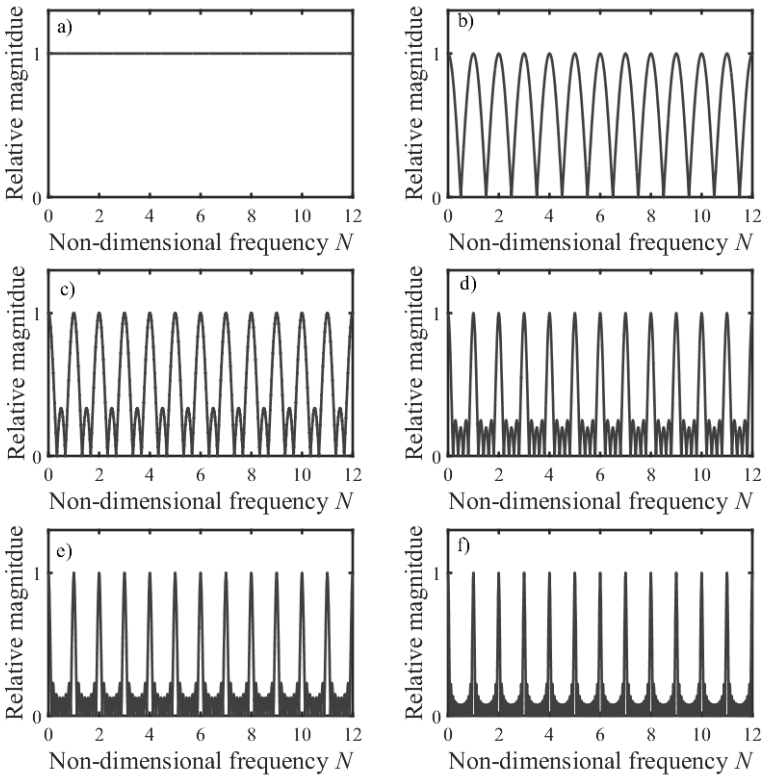

Fig. 7. Effect of increasing the number of vehicles in a train on the series in Eq.(9): series length of: a) 1 vehicle; b) 2 vehicles; c) 3 vehicles; d) 5 vehicles; e) 8 vehicles; f) 13 vehicles.

The full load spectrum determined from Eq. (9) is shown in Fig. 8 for trains comprising Javelin vehicles. As this combines the results in Figs 6 and 7, the spectral peaks do not occur exactly at integer multiples of the vehicle passing frequency, especially for short trains. However, as the number of vehicles increases, the peaks in Fig. 8 increase in sharpness and tend to integer multiples of the vehicle passing frequency, owing to the sharpness of the peaks in Fig. 7.

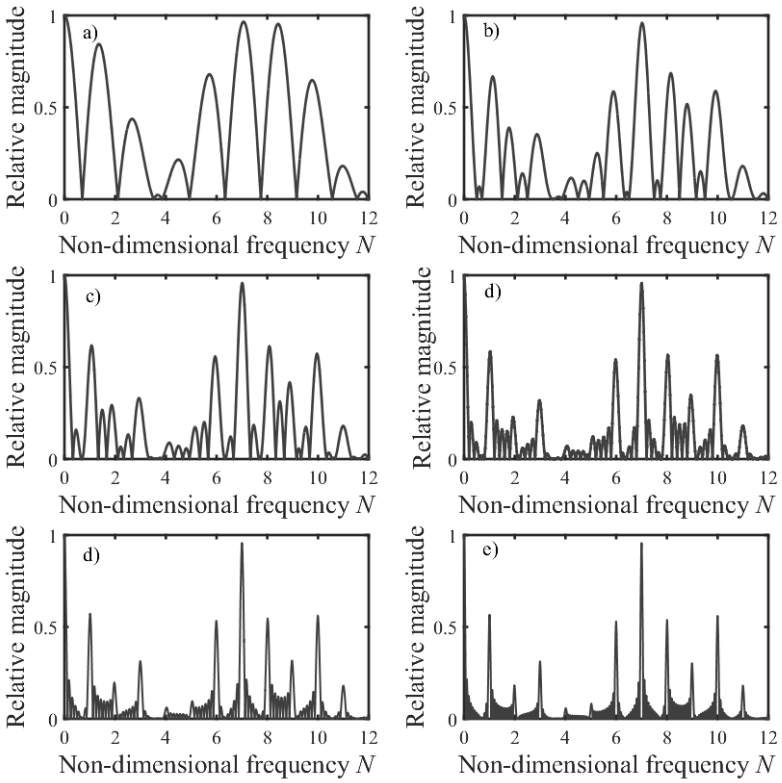

Fig. 8. Train load spectrum for a train of 20 m Javelin vehicles comprising: a) 1 vehicle; b) 2 vehicles; c) 3 vehicles; d) 5 vehicles; e) 8 vehicles; f) 13 vehicles.

Fig. 9 shows the relative magnitude of the Fourier transform calculated using Eq. (9) for a 6 car Javelin, 5 car Voyager, 11 car Pendolino and 16 car Valero (Fig 2). The weighting functions according to Eq. (8), that form an envelope for the spectra are also shown.

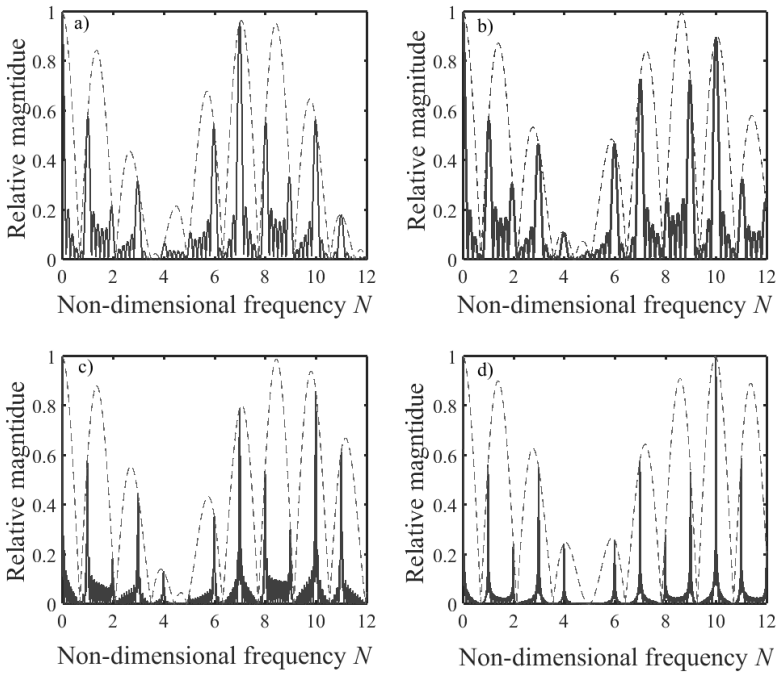

Fig. 9. Relative magnitude of the Fourier transform for the train loads for multiple car from Eq. (9) (—), weighting due to to vehicle geometry from Eq. (8) (- -), for a) 6 vehicle Javelin; b) 5 vehicle Voyager; c) 11 vehicle Pendolino; d) 16 vehicle Valero.

In Fig. 9 the spectral peaks occur at frequencies that are very close to integer multiples of the vehicle passing frequency for each example. The relative magnitudes of these peaks are modulated by weighting function. This means that Eq. (8) can be used to determine the magnitude of the vehicle passing frequencies for periodic trains from vehicle geometry alone, provided that the difference between the actual and the nominal frequencies has a small effect on the magnitude. These differences will be considered in section 4.2.

3.4. *Non-periodic trains*

3.4.1.Effect of multiple vehicle types

The HST (see Fig. 3(a)) comprises vehicles of two different lengths. Fig. 10 shows the train load spectra obtained (a) for a train consisting of the primary vehicles only, and (b) for the entire train. When there is only a single vehicle type (Fig. 10(a)), the train load spectrum has the properties of a periodic train: spectral peaks are multiples of the vehicle passing frequency and their relative amplitudes can be calculated using Eq. (8). The inclusion of power cars changes the spectrum (Fig. 10(b)): the spectral peaks remain close to integer multiples of the vehicle passing frequencies but their magnitudes are reduced and cannot be calculated using Eq. (8).

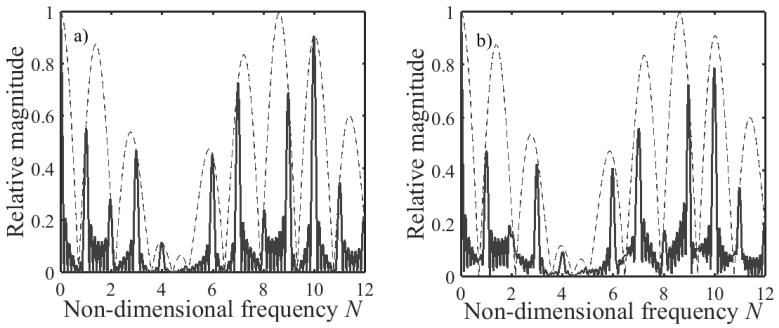

Fig. 10. Relative magnitude of the Fourier transform for the train loads from a) 7 Mk3 coaches and b) 9 vehicle HST. Train load spectrum (─), weighting due to vehicle geometry (···).

3.4.2.Effects of coupling trainsets together

Trainsets are often coupled to form longer trains, for example the 12-car (i.e. 2×6 car) Javelin (Fig. 3(b)). The coupling length between trainsets may be different from the coupling length between vehicles within a trainset. This introduces a phase shift between trainsets, which can cause localised suppressions as in Fig. 11, which shows simulated results for coupled Javelin trainsets. This can also lead to twin peaks, shown close to the 7th harmonic of the vehicle passing frequency, in the insert within Fig. 11.

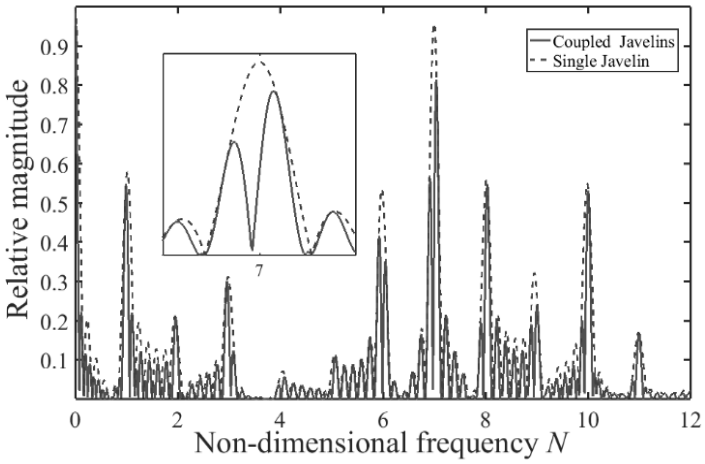

Fig. 11. Relative magnitude of the Fourier transform for the train loads from a six vehicle Javelin trainset (- -), and two six vehicle trainsets with an additional coupling length of 1.4 m (--).

The Fourier transform for two coupled trainsets $F_c(N)$, can be written as the Fourier transform for the single trainset $F(N)$, together with a phase shift:

$$F_c(N) = F(N)\left(1 + \mathrm{e}^{\frac{-\mathrm{i}2\pi N(L_t+L_c)}{L_v}}\right) \tag{10}$$

where L_t is the trainset length and L_c is the additional coupling length. The effect on the spectrum depends on the phase difference introduced by the coupling between the two trainsets.

3.4.3.Effects of multiple vehicle lengths and coupling

The Class 373 Eurostar consists of two coupled trainsets of 10 vehicles each (Fig. 3(c)); each trainset contains three different vehicle types: seven articulated passenger vehicles, two semi-articulated passenger vehicles, and a powered driving vehicle with conventional bogies. Fig. 12 shows the relative magnitudes for the nine articulated vehicles, a single trainset and two coupled trainsets forming a complete 20 car train. When only the passenger vehicles are considered the train has a periodic structure, the spectral peaks are at the multiples of the vehicle passing frequency and their amplitudes can be obtained from Eq. (8) (Fig. 12(a)). For these articulated vehicles, the weighting function depends only on the axle spacing. As before, the introduction of a vehicle of different geometry changes the spectrum (Fig. 12(b)) and the magnitudes of the peaks are reduced. Coupling two trainsets changes the spectrum further (Fig. 12(c)), but the spectral peaks remain close to multiples of the primary vehicle passing frequency. The complete trainset geometry needs to be considered to determine the magnitudes of the dominant train load frequencies for trains that contain multiple vehicle types or coupled trainsets.

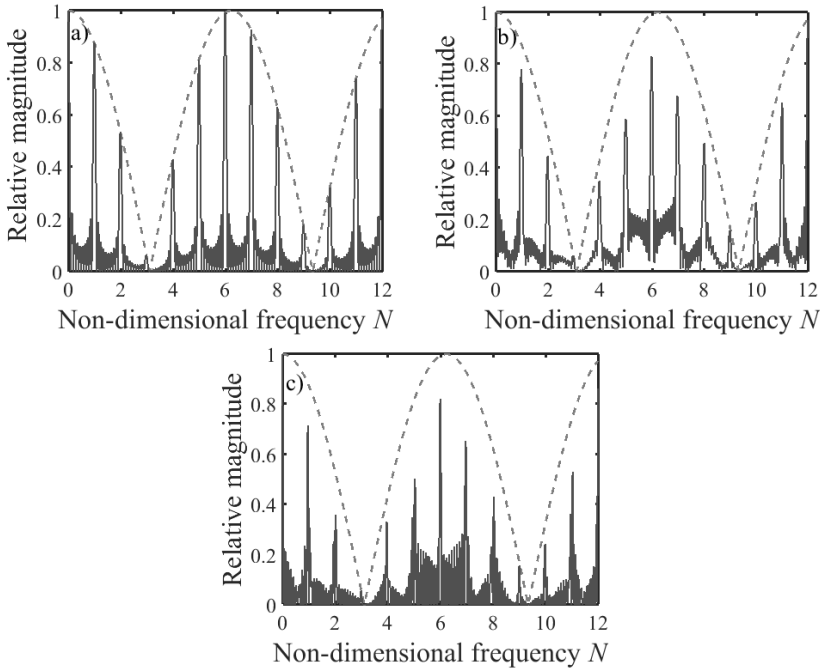

Fig. 12. Relative magnitude of the Fourier transform for the train loads from: a) the passenger saloons in a Class 373 Eurostar trainset; b) drive car and passenger saloons in a single Eurostar trainset; c) two coupled Eurostar trainsets. Train load spectrum (—), weighting due to vehicle geometry (- -).

4. Applications

A knowledge of which frequencies may be expected to be prominent or suppressed in spectra of track vibration can be used to verify whether the track is behaving normally or has some unexpected behaviour [5]. As previous authors have noted [2, 8-10] the information can also be used to determine train speeds. These properties can be combined with track models in the frequency domain to interpret the behaviour of the track. Calculation of the relative magnitude of spectral peaks for loading has been

used to interpret track-based measurements by obtaining the track system support modulus without knowing the applied load [5]. Also, the properties of the train load spectrum and the track model provide a basis for identifying optimal frequencies for tuning energy harvesting devices to gather energy from track deflections [6]. These applications are discussed briefly in the following sections, with reference to 'periodic' trains having a single vehicle type.

4.1. *Obtaining track system support modulus*

Track stiffness is often taken as a proxy for track quality. It is often evaluated from time histories of deflection measured at the rail or on a sleeper together with information about the loads. Thus measurements of displacement and load are required, as well as a knowledge of vehicle geometry [26, 27]. In practice the first two can be difficult to obtain with certainty. A closed form solution can be obtained from the beam-on-elastic-foundation model, allowing the track system support modulus to be determined from the ratio of amplitudes of two spectral peaks of the measured rail vibration [5]. The properties of the train load spectra explored in this paper can be used to show that this method can be applied using the geometry of a single vehicle rather than that of the whole train. Moreover, a more rigorous justification will be given for the pair of frequencies selected for evaluation.

In the method proposed in [5], a pair of spectral peaks with non-dimensional frequencies N_a and N_b, assumed to be integer multiples of the vehicle passing frequency, are identified in a spectrum of track displacement, velocity or acceleration. The ratio W_r between the amplitudes at these peaks is found. According to Eq. (7) these amplitudes are the product of the shape and load spectra, Eq. (4) and Eq. (8) the latter depending on the track support stiffness. For trains having a periodic structure, the ratio between the amplitudes of these peaks in the train load spectrum can be calculated from the geometry of the vehicle rather than that of the train. Thus the result from [5] can be expressed as:

$$W_r\left(\frac{N_\mathrm{a}}{N_\mathrm{b}}\right) = \frac{kL_v^4 + 16\pi^4 EI{N_\mathrm{b}}^4}{kL_v^4 + 16\pi^4 EI{N_\mathrm{a}}^4} \cdot \frac{\cos\left(\frac{\pi N_\mathrm{a} L_b}{L_v}\right)\cos\left(\frac{\pi N_\mathrm{a} L_w}{L_v}\right)}{\cos\left(\frac{\pi N_\mathrm{b} L_b}{L_v}\right)\cos\left(\frac{\pi N_\mathrm{b} L_w}{L_v}\right)} \tag{11}$$

The corresponding equations for velocity and acceleration may be obtained by multiplying Eq. (11) by N_a/N_b and N_a^2/N_b^2, respectively. This result is independent of wheel load and train speed. As EI for the rail is known, only the vehicle geometry is required to calculate the track system support modulus.

4.2. *Frequency selection*

The pair of frequencies selected for evaluation can affect the success of the approach. The spectral peaks used should be prominent in both the measured and the theoretical trainload spectrum, be accurately and reliably obtained from the vehicle geometry, insensitive to variations in wheel load, should not be too close to one another so that good resolution can be achieved and account for transducer performance.

4.2.1.Approximating the relative amplitudes of dominant train load frequencies

For any train with a single vehicle type and equal loads the train load spectra are weighted by the function of vehicle geometry given in Eq. (8). If there are sufficient vehicles in the train, the spectral peaks occur at approximately integer multiples of the vehicle passing frequency. Eq. (8) can thus be used to determine the amplitudes of these peaks in the load spectrum.

However, as shown in Fig. 9, for shorter trains the peaks will be broader and there will be a difference between the actual and the nominal frequencies (nearest integer multiple) of the peaks. This difference in frequency also affects the relative magnitudes, as shown in Fig. 13 for the example of a Javelin with an increasing number of vehicles. The difference between the actual frequency and the nominal frequency is expressed as a percentage of the vehicle passing frequency; the difference between the actual amplitude and the nominal amplitude for each peak is expressed as a percentage of the nominal amplitude. All these results are shown as positive to allow a logarithmic scale to be used. Similar trends are obtained for the other vehicle geometries.

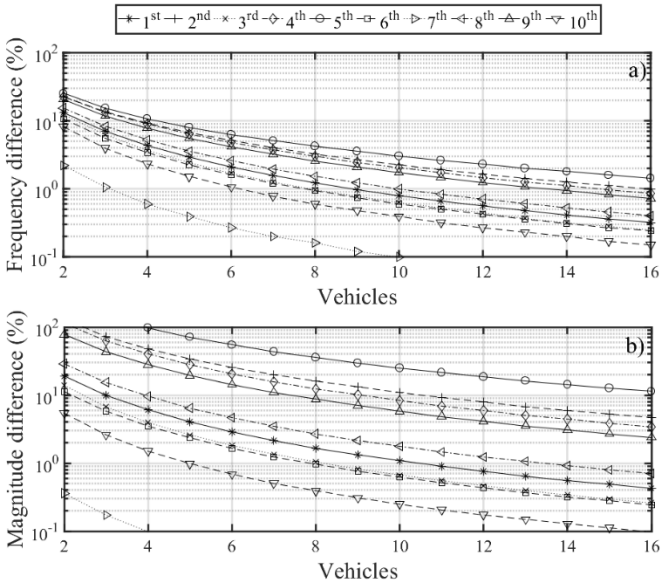

Fig. 13. Relative differences between (a) nominal and (b) actual frequency and magnitude of spectral peaks in the train load spectrum for a Javelin train with different numbers of vehicles.

The differences in Fig. 13 vary from one peak to another, depending on whether the peak is near a local maximum or a zero in the single vehicle spectrum. If a nominal frequency is near to a maximum in the single vehicle spectrum, for example the 1st, 3rd, 6th, 7th and 10th nominal frequencies in the present case (see Fig. 7) the spectral peak will be well-defined for any number of vehicles and there will be only a small difference between the actual and nominal peaks. Although the 8th nominal frequency has a similar magnitude to the 6th in Fig. 7, the 6th is closer to the local maximum and therefore subject to a smaller error in Fig. 14. If a peak is near a suppressed frequency, for example the 2nd and 5th nominal frequencies, it will be subject to greater error and as it cannot be prominent it should not be used in evaluating track stiffness. From Fig. 10 it can be seen that the 1st, 3rd, 6th 7th and 10th nominal

frequencies are close to local maxima in the single vehicle spectrum for all the trains studied, whereas the 2nd and 5th nominal frequencies tend to be suppressed. Others vary between train types. The error at 1st, 3rd, 6th 7th and 10th nominal frequencies is less than ±3% of the vehicle passing frequency provided that the train has five or more vehicles.

4.2.2.Effects of variation in wheel load

In this analysis it has been assumed that all wheel loads are equal. In reality there will be some variation between wheel loads owing to differences between vehicle equipment, occupancy and dynamic loading effects. Ju et al. [17] showed that, when rail irregularities cause variation between wheel loads, the *frequencies* of the dominant peaks are stable. In this section the effect of variations in wheel load on the *magnitude* of the train load spectrum is considered. Measured static axle loads for 99 Javelin trainsets passing a weighing-in-motion system were found to have a relative standard deviation of the axle load of about 4%. Dynamic effects are likely to increase this variation.

In Monte-Carlo simulations of 1000 notional trains, each wheel load was modelled as a normally distributed random variable with a standard deviation of 4, 5, 10 and 20% of the mean. The track deflections were obtained in the time domain from the beam model and the spectrum was obtained using a discrete Fourier transform. The variation in wheel load changes the train load spectra and causes magnitude of the spectral peaks to vary. The frequency did not change, see also [17]. Fig. 14 shows the relative standard deviation of the magnitude of the spectral peaks for a 4% variation. These are expressed relative to the actual magnitude obtained for equal loads rather than to the nominal magnitude, so the errors are in addition to those in Fig. 13. For higher variations in wheel load, these results increase in proportion to the standard deviation of the wheel load.

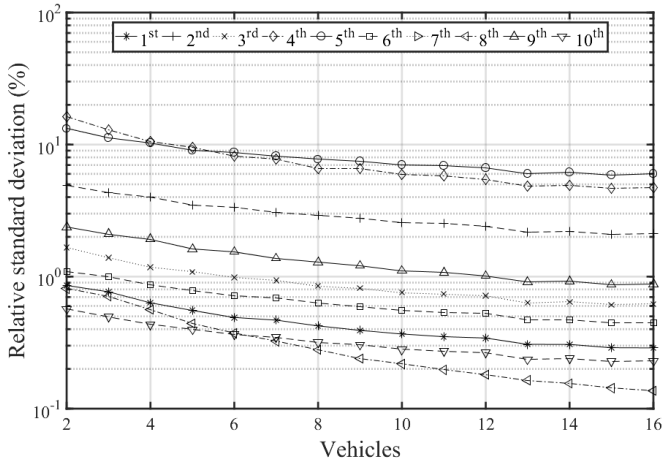

Fig. 14. Variation of the expected magnitude at each spectral peak for a train consisting of increasing numbers of Javelin vehicles; each wheel load was modelled as a normally distributed random variable with a standard deviation of 4% of the mean load.

The relative standard deviation was found to vary from one peak to another. For this example of the Javelin, the effects were smallest at the 1st, 3rd, 6th, 7th and 10th nominal frequencies, which are again the dominant frequencies closest to local maxima in the single vehicle spectrum. The relative

standard deviation for the 7th nominal frequency was less than 0.1% and therefore not visible on the graph. For each simulated load variation, the relative standard deviation of the peaks was less than half the specified relative standard deviation of the axle loads, for all train lengths studied, and reduced as the train length was increased. These results show that, for a typical variation in axle load, the effect on the magnitude of the 1st, 3rd, 6th, 7th and 10th nominal frequencies was less than 2%. The magnitudes of these peaks may therefore be calculated accurately using Eq. (8).

4.2.3.Track model resolution

For a pair of frequencies to be suitable for use in Eq. (11), it is also important that the amplitude ratio discriminates between different values of track system support modulus. Fig. 15 illustrates the sensitivity to the track system support modulus of the ratio between the amplitudes of various pairs of frequencies for the Javelin. This corresponds to the first term in Eq. (11). The plausible range of track system support modulus is also indicated. Increased separation between peaks increases the sensitivity of the function to the track system support modulus. This suggests a ratio of the 10th or 7th to the 1st or 3rd vehicle passing frequencies would be most suitable for determining the track system support modulus in this example.

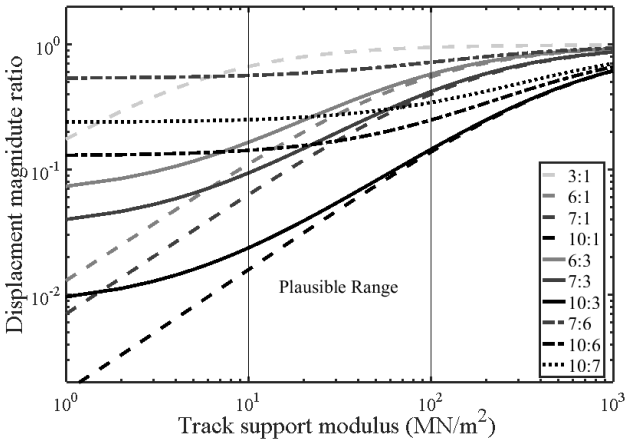

Fig. 15. Magnitude ratio between different pairs of frequencies (multiples of vehicle passing frequency) for a 20 m vehicle, obtained from shape function (track displacement from the beam on elastic foundation model) for varying track system support modulus and a single UIC 60 rail.

4.2.4. Signal amplitude and frequency range

Obtaining a reliable measurement will depend on the amplitude of the peak and transducer performance. A low amplitude signal will be more sensitive to transducer noise. This is a particular concern for lower cost transducers [24]. Choosing higher amplitude peaks will improve the signal to noise ratio, enabling low cost transducers to be used for track vibration measurements. Low frequency peaks, i.e. the 1st harmonic, should be avoided when using velocity or acceleration transducers as the signal will be low amplitude. Higher frequency peaks may approach an actual frequency of 30-40 Hz for faster trains. These are more likely to be affected by dynamic excitation due to track unevenness or wheel out of roundness and should be avoided in the analysis.

4.3. *Example*

The factors discussed in section 4.2 have been used to select a pair of dominant frequencies for evaluating Eq. (11) for a Javelin. As noted above, the 1st, 3rd, 6th, 7th and 10th harmonics of the vehicle passing frequency are prominent for the in Fig. 9(b), they are calculated accurately using vehicle geometry and are insensitive to variations between wheel loads (Fig. 14). The 7th harmonic is the most reliable peak. The 1st harmonic was less sensitive to load variability than the 3rd, but less accurately calculated using Eq. (8) as it was more sensitive to the number of vehicles in the train (Fig. 13(a)). Furthermore, the 1st harmonic occurs at a low frequency (< 4 Hz) and thus is likely to have a low magnitude if measured as a velocity or acceleration. The ratios of the 7th to the 3rd or the 10th to the 3rd harmonics appear to be suitable. However, the 10th harmonic may be more influenced by dynamic excitation. For these reasons the ratio of the 7th and 3rd harmonics is the most suitable for determining the track system support modulus in the frequency domain for the Javelin. This ratio was found to be appropriate for the other periodic trains studied for similar reasons, as proposed in [5].

For a given pair of frequencies, the vehicle geometry can be used to compute calibration curves expressing the expected magnitude ratio as a function of track system support modulus for track displacement using Eq. (11), or the equivalent for velocity or acceleration. Example curves for the expected displacement magnitude ratio between the 7th and 3rd harmonics of the vehicle passing frequency for the four periodic trains studied are given in Fig. 16. The differences between the curves are caused by the vehicle geometry and correspond to the differences seen in Fig. 9.

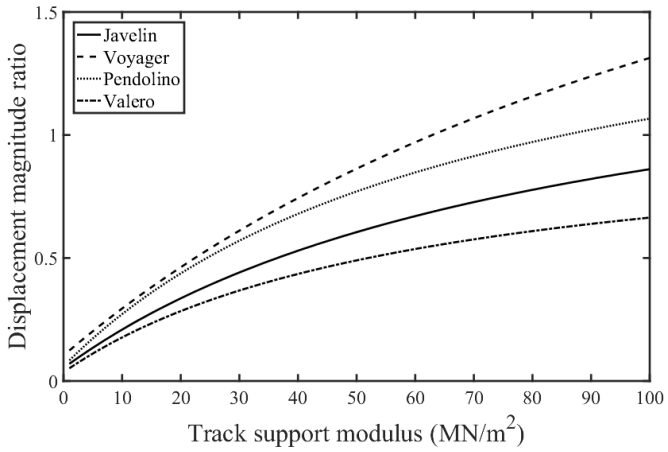

Fig. 16. Expected displacement magnitude ratio between the 7th and 3rd vehicle passing frequencies for different train types for a plausible range of track system support modulus and a single UIC 60 rail.

The curves in Fig. 16 have been used to obtain track support moduli for each set of measurements in Fig. 2, each train is from a different location. These are given in Table 2 and all are plausible results for track system support modulus.

Table 2 Track system support modulus found using the ratios of the magnitdue at the 7th and 3rd harmonics of the vehcile passing frequency from track-based measurements.

Trainset	7th (m/s/Hz)	3rd (m/s/Hz)	Velocity Ratio	Displacement Ratio	Modulus (MN/m^2)
Voyager	0.0187	0.0164	1.14	0.49	35
Javelin	0.0261	0.0170	1.54	0.66	35
Pendolino	0.0133	0.0106	1.26	0.54	27
Valero	0.0195	0.0215	0.91	0.39	35

For the Javelin trains, this result can be compared with estimates obtained from measurements of static wheel loads and peak dynamic loads obtained from a weighing-in-motion system, which should form lower and upper bounds for actual loads. A displacement of 0.35 mm was obtained by integrating sleeper velocity measurements using the method given in [19]. The mean measured wheel loads for the train studied were 54 kN static and 74 kN total load (including the peak dynamic contribution from wheel out of roundness). After accounting for the rail pad stiffness of 70 MN/m, these give track system support moduli of 32.3 and 37.6 MN/m^2 respectively. The track system support modulus obtained from the frequency domain method was 35 MN/m^2 which is within the range of values calculated for possible wheel loads using the direct method.

The difference between average measured static and dynamic wheel loads was significant (up to 30%), resulting in calculated values of track system support modulus that varied by 16.4%. This is typical of the uncertainty associated with calculating the track system support modulus directly from a load and a measured displacement. Obtaining the track system support modulus using the frequency domain method overcomes much of this uncertainty as the exact load is not needed.

4.4. *Determining train speed*

Train speed can be determined from line side measurements from a single transducer mounted on the track superstructure in different ways:

1. In the frequency domain by determining the vehicle passing frequency found from the average of multiple peaks and then multiplying by the vehicle length [2, 8]. The accuracy can be improved by interpreting the data with reference to a ground vibration model [9].
2. In the frequency domain by determining the vehicle passing frequency using a single reliable peak and then multiplying by the vehicle length.
3. In the time domain by determining the time between deflections under individual wheel loading separated by a known vehicle or trainset length.

Speeds found using these three methods are summarised in Table 3. The 7th harmonic was used for the single peak approach.

Table 3 Train speeds determined using a single spectral peak, multiple peaks and in the time domain

Trainset	Train speed (m/s)		
	Multiple Peaks	Single Peak (7^{th} harmonic)	Time domain
Javelin	56.5	56.4	56.1
Voyager	56.2	56.1	56.3
Pendolino	54.3	54.4	53.9
Velaro	80.8	80.8	80.4

The accuracy of the frequency domain approaches depends on whether the actual frequency of a spectral peak corresponds to an exact multiple of the vehicle passing frequency, which varies from peak to peak (Fig. 13(a)). Thus it is likely to be more accurate (or at least quicker) to identify the vehicle passing frequency from a spectral peak that theoretically always occurs at an integer multiple of the vehicle passing frequency (Fig. 13) and is not influenced by variation in wheel load (Fig. 14.), rather than find an average speed using many peaks. The difference between using an appropriate single reliable peak and the average speed from many peaks was less than 0.4% for the trains in section 2. The differences between the estimates obtained in the time and the frequency domain were less than 1% suggesting that the methods are of similar accuracy for measurements taken on the track superstructure.

4.5. *Tuning of energy harvesters*

For continuous remote condition monitoring, track-mounted transducers are ideally powered using energy harvesting devices, commonly single-degree-of-freedom systems that require tuning to optimise energy abstraction. Trainload frequencies can be used to determine the appropriate energy harvesting frequencies for known vehicle types and train speeds.

The optimum amount of energy harvested by a single-degree-of-freedom harvester is proportional to the product of the squares of the input acceleration amplitude and the input duration [6]. To optimise energy abstraction from track deflections due to passing trains, an energy harvesting device should therefore be tuned to a frequency corresponding to a peak in the acceleration spectrum.

The Fourier transform of the acceleration obtained from the beam-on-elastic-foundation model can be used to determine where the acceleration spectrum due to a single moving load has a maximum. The magnitude of the Fourier transform of the acceleration due to a unit load can be found from Eq. (8). This has a maximum that can be expressed as a non-dimensional frequency for a given vehicle length:

$$N = \frac{L_v}{2\pi}\sqrt[4]{\frac{k}{EI}} \tag{12}$$

This varies with track system support modulus for a given rail section. However, this frequency may not correspond to a peak in the train load spectrum as the vehicle geometry will cause certain frequencies to be suppressed. Thus it necessary to find a large prominent peak in the acceleration spectrum, accounting for vehicle geometry. This will be the global maximum of:

$$A(N) = \frac{4\pi^4 L_v^4 N^2 v}{kL_v^4 + 16EIN^4\pi^4}\left|\cos\left(\frac{\pi N L_b}{L_v}\right)\cos\left(\frac{\pi N L_w}{L_v}\right)\right| \tag{13}$$

Fig. 17 shows the magnitude of this function at different non-dimensional frequencies for different track support moduli for the Javelin vehicle geometry. The darker regions indicate higher accelerations than the lighter regions.

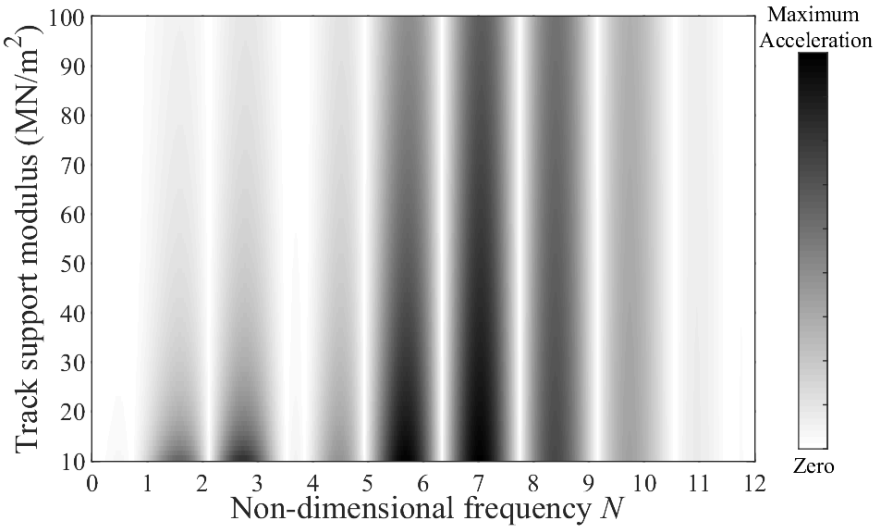

Fig. 17. Map of acceleration spectrum against non-dimensional frequency for a 20 m vehicle

This analysis can be used to identify the optimal frequency for a particular vehicle type. An energy harvester can then be tuned to the optimal frequency for a given line speed. For the trains considered in this study the acceleration is greatest in the region of the 7th harmonic, except for the Eurostar for which the 6th is most significant. This corresponds to frequencies of 21 Hz for the Javelin and the Velaro, assuming typical operating speeds of 60 and 75 m/s, 24 Hz for a Eurostar also at 75 m/s, and 16.7 Hz for a Voyager or an HST and 16.1 Hz for a Pendolino (all at 55 m/s).

5. Conclusions

1. Using track vibration measurements and a model for train loads and track deflection, it has been shown that the most prominent spectral peaks occur at frequencies close to integer multiples of the vehicle passing frequency. For periodic trains consisting of a single vehicle type, the train load spectrum depends on the vehicle geometry and the number of vehicles. It has further been shown that the spectral peaks tend to integer multiples of the vehicle passing frequency as the number of vehicles increases. The relative magnitudes of these peaks are weighted by a function equivalent to the spectrum for a single vehicle. This function depends on the vehicle geometry and will define the overall envelope of the train load spectrum, regardless of the number of vehicles in the train.
2. The number of vehicles affects how closely the spectral peaks occur to multiples of the vehicle passing frequency. Provided that a train has five or more vehicles, the Fourier series for an infinite train can be used to approximate the relative amplitudes of spectral peaks to within ± 3% of the result for the complete train geometry. For trains that have multiple vehicle types with one type

dominant, the spectral peaks also occur at multiples of the passing frequency of the dominant vehicle, but the complete train geometry is required to determine their magnitude.

3. The properties of the peaks in a train loading spectrum can be used to determine the track system support modulus by fitting a model of track deflections in the frequency domain, and analysing the measured amplitude ratio of a pair of spectral peaks. Certain spectral peaks have been shown to be more appropriate for this approach than others. Whether a peak is prominent in the spectrum depends on the vehicle geometry; certain frequencies are suppressed because of the axle and bogie spacing within a vehicle. The pair of peaks selected should also be sufficiently separated for their ratio to be sensitive to changes in the track system support modulus. Peaks expected at the 3rd and 7th multiples of the vehicle passing frequency have been shown to meet both criteria for a range of common UK vehicle geometries. The frequency domain approach reduces uncertainty in the track system support modulus compared with other methods as the wheel loads are not required for the calculation. The method also enables the track system support modulus to be determined from data obtained using a single transducer.
4. Train speed can be determined from track vibration measurements in the frequency domain by identifying the frequency of a single prominent peak known to occur reliably at a multiple of the vehicle passing frequency. The 7th harmonic is appropriate for most of the trains considered. The same property can be used for tuning track based energy harvesting devices. These should be tuned to the frequency of greatest acceleration to maximise energy extraction. Track models indicate the corresponding frequency for a given line speed. However, unless this corresponds to a spectral peak from the loading there will be little energy to gather. Energy harvesting devices should be tuned to the most prominent train load spectral peak in the vicinity of the frequency where the acceleration spectrum has its maximum. For common trains operating at typical line speeds on the UK rail network, this was found to occur between 16 and 21 Hz.

6. Acknowledgements

The research was funded by the Engineering and Physical Sciences Research Council (EPSRC) through the research grant *Track Systems for High Speed Railways: Getting It Right* (EP/K03765X), the *Industry Doctoral Training Centre in Transport and the Environment* (EP/G036896/1) and the programme grant *Track to the Future* (EP/M025276/1). This work would also not have been possible without the kind assistance and advice given by Mick Hayward and Simon Morley of Network Rail High Speed. Geoff Watson, Martin Toward and Taufan Abadi of the University of Southampton assisted with the work. All data supporting this study are openly available from the University of Southampton repository at http://dx.doi.org/10.5258/SOTON/D0018.

7. References

[1] L. Auersch, The excitation of ground vibration by rail traffic: theory of vehicle–track–soil interaction and measurements on high-speed lines, *Journal of Sound and Vibration*, 284 (2005) 103-132.
[2] S.-H. Ju, H.-T. Lin, J.-Y. Huang, Dominant frequencies of train-induced vibrations, *Journal of Sound and Vibration*, 319 (2009) 247-259.
[3] G. Kouroussis, D.P. Connolly, O. Verlinden, Railway-induced ground vibrations – a review of vehicle effects, *International Journal of Rail Transportation*, 2 (2014) 69-110.
[4] X. Bian, H. Jiang, C. Chang, J. Hu, Y. Chen, Track and ground vibrations generated by high-speed train running on ballastless railway with excitation of vertical track irregularities, *Soil Dynamics and Earthquake Engineering*, 76 (2015) 29-43.
[5] L. Le Pen, D. Milne, D. Thompson, W. Powrie, Evaluating railway track support stiffness from trackside measurements in the absence of wheel load data, *Canadian Geotechnical Journal*, 53 (2016) 1156-1166.
[6] G. Gatti, M.J. Brennan, M.G. Tehrani, D.J. Thompson, Harvesting energy from the vibration of a passing train using a single-degree-of-freedom oscillator, *Mechanical Systems and Signal Processing*, 66–67 (2016) 785-792.
[7] L. Auersch, Ground vibration due to railway traffic—The calculation of the effects of moving static loads and their experimental verification, *Journal of Sound and Vibration*, 293 (2006) 599-610.
[8] S.-H. Ni, Y.-H. Huang, K.-F. Lo, An automatic procedure for train speed evaluation by the dominant frequency method, *Computers and Geotechnics*, 38 (2011) 416-422.
[9] G. Kouroussis, D.P. Connolly, M. Forde, O. Verlinden, Train speed calculation using ground vibrations, *Proceedings of the Institution of Mechanical Engineers, Part F: Journal of Rail and Rapid Transit*, 229 (2013) 466-483.
[10] V. Jurdic, O. Bewes, K. Burgnemeister, D.J. Thompson, *Train speed estimations from ground vibration measurements using a simple rail deflection model mask*, in: 12th International Workshop on Railway Noise, Terrigal, Australia, 2016.
[11] K.L. Knothe, S.L. Grassie, Modelling of Railway Track and Vehicle/Track Interaction at High Frequencies, *Vehicle System Dynamics*, 22 (1993) 209-262.
[12] X. Sheng, C.J.C. Jones, D.J. Thompson, A comparison of a theoretical model for quasi-statically and dynamically induced environmental vibration from trains with measurements, *Journal of Sound and Vibration*, 267 (2003) 621-635.
[13] X. Sheng, C.J.C. Jones, D.J. Thompson, A theoretical study on the influence of the track on train-induced ground vibration, *Journal of Sound and Vibration*, 272 (2004) 909-936.
[14] G. Lombaert, G. Degrande, J. Kogut, S. François, The experimental validation of a numerical model for the prediction of railway induced vibrations, *Journal of Sound and Vibration*, 297 (2006) 512-535.
[15] N. Triepaischajonsak, D.J. Thompson, C.J.C. Jones, J. Ryue, J.A. Priest, Ground vibration from trains: experimental parameter characterization and validation of a numerical model, *Proceedings of the Institution of Mechanical Engineers, Part F: Journal of Rail and Rapid Transit*, 225 (2011) 140-153.
[16] P. Alves Costa, R. Calçada, A. Silva Cardoso, Track–ground vibrations induced by railway traffic: In-situ measurements and validation of a 2.5D FEM-BEM model, *Soil Dynamics and Earthquake Engineering*, 32 (2012) 111-128.
[17] S.H. Ju, J.R. Liao, Y.L. Ye, Behavior of ground vibrations induced by trains moving on embankments with rail roughness, *Soil Dynamics and Earthquake Engineering*, 30 (2010) 1237-1249.
[18] G. Lombaert, G. Degrande, S. François, D.J. Thompson, *Ground-Borne Vibration due to Railway Traffic: A Review of Excitation Mechanisms, Prediction Methods and Mitigation Measures*, in: J.C.O. Nielsen, D. Anderson, P.-E. Gautier, M. Iida, J.T. Nelson, D. Thompson, T. Tielkes, D.A. Towers, P. de Vos (Eds.) Noise and Vibration Mitigation for Rail Transportation Systems, Springer Berlin Heidelberg, 2015, pp. 253-287.
[19] D. Bowness, A.C. Lock, W. Powrie, J.A. Priest, D.J. Richards, Monitoring the dynamic displacements of railway track, *Proceedings of the Institution of Mechanical Engineers, Part F: Journal of Rail and Rapid Transit*, 221 (2007) 13-22.

[20] F. Lamas-Lopez, V. Alves-Fernandes, Y.J. Cui, S. Costa D'Aguiar, N. Calon, J.C. Canou, A.M. Tang, A. Roubinet, *Assessment of the double Integration method using accelerometers data for conventional railway platforms*, in: J. Pombo (Ed.) Proceedings of the second international conference on railway technology: Research, development and maintenance, Civil-Comp Press, Ajaccio, 2014.
[21] L. Le Pen, G. Watson, W. Powrie, G. Yeo, P. Weston, C. Roberts, The behaviour of railway level crossings: Insights through field monitoring, *Transportation Geotechnics*, 1 (2014) 201-213.
[22] D. Mishra, Y. Qian, H. Huang, E. Tutumluer, An integrated approach to dynamic analysis of railroad track transitions behavior, *Transportation Geotechnics*, 1 (2014) 188-200.
[23] J.A. Priest, W. Powrie, L.A. Yang, P.J. Grabe, C.R.I. Clayton, Measurements of transient ground movements below a ballasted railway line, *Géotechnique*, 60 (2010) 667-677.
[24] D. Milne, L. Le Pen, G. Watson, D. Thompson, W. Powrie, M. Hayward, S. Morley, Proving MEMS Technologies for Smarter Railway Infrastructure, *Procedia Engineering*, 143 (2016) 1077-1084.
[25] L. Frýba, *Vibration of solids and structures under moving loads*, Noordhoff, Groningen, The Netherlands, 1972.
[26] A.D. Kerr, On the determination of the rail support modulus k, *International Journal of Solids and Structures*, 37 (2000) 4335-4351.
[27] S. Timoshenko, B.F. Langer, Stresses in railroad track, *ASME Transactions*, 54 (1932) 277-293.